Brain Topogr (2010) 23:243–256
DOI 10.1007/s10548-010-0147-9

ORIGINAL PAPER

Neuroelectrical Hyperscanning Measures Simultaneous Brain Activity in Humans

Laura Astolfi · Jlenia Toppi · Fabrizio De Vico Fallani · Giovanni Vecchiato · Serenella Salinari · Donatella Mattia · Febo Cincotti · Fabio Babiloni

Received: 18 March 2010 / Accepted: 5 May 2010 / Published online: 18 May 2010

Abstract In this study we illustrate a methodology able to follow and study concurrent and simultaneous brain processes during cooperation between individuals, with non invasive EEG methodologies. We collected data from fourteen pairs of subjects while they were playing a card game with EEG. Data collection was made simultaneously on all the subjects during the card game. An extension of the Granger-causality approach allows us to estimate the functional connection between signals estimated from different Regions of Interest (ROIs) in different brains during the analyzed task. Finally, with the use of graph theory, we contrast the functional connectivity patterns of the two players belonging to the same team. Statistically significant functional connectivities were obtained from signals estimated in the ROIs modeling the anterior cingulate cortex (ACC) and the prefrontal areas described by the Brodmann areas 8 with the signals estimated in all the other modelled cortical areas. Results presented suggested the existence of Granger-sense causal relations between the EEG activity estimated in the prefrontal areas 8 and 9/46 of one player with the EEG activity estimated in the ACC of their companion. We illustrated the feasibility of functional connectivity methodology on the EEG hyperscannings performed on a group of subjects. These functional connectivity estimated from the couple of brains could suggest, in statistical and mathematical terms, the modelled cortical areas that are correlated in Granger-sense during the solution of a particular task. EEG hyperscannings could be used to investigate experimental paradigms where the knowledge of the simultaneous interactions between the subjects have a value.

Keywords EEG hyperscanning · Partial Directed Coherence · Functional connectivity

L. Astolfi · F. De Vico Fallani · G. Vecchiato · D. Mattia · F. Cincotti · F. Babiloni (✉)
IRCCS "Fondazione Santa Lucia", Rome, Italy
e-mail: fabio.babiloni@uniroma1.it

L. Astolfi
e-mail: laura.astolfi@uniroma1.it

F. De Vico Fallani
e-mail: fabrizio.devicofallani@uniroma1.it

G. Vecchiato
e-mail: giovanni.vecchiato@uniroma1.it

D. Mattia
e-mail: d.mattia@hsantalucia.it

F. Cincotti
e-mail: f.cincotti@hsantalucia.it

L. Astolfi · J. Toppi · S. Salinari
Department of Computer and Systems Science, University "Sapienza", Rome, Italy

J. Toppi
e-mail: jlenia.toppi@uniroma1.it

S. Salinari
e-mail: salinari@dis.uniroma1.it

F. De Vico Fallani · G. Vecchiato · F. Babiloni
Department of Physiology and Pharmacology, University "Sapienza", Rome, Italy

Introduction

Although one of the most relevant characteristics of human behavior is the cooperation between individuals (Lee and DeVore 1968; Whiten and Byrne 1988), little is known about the neural substrates that implement such attribute during "*de visu*" (i.e., face to face) performances. This is due also to the technical difficulty of the brain imaging techniques to track simultaneously different human brains

during cooperative interactions (King-Casas et al. 2005). A major limitation of the approach used in the majority of the studies described above, is that the neural activity, during social interaction, is actually measured in only one of the participating brains. The "interaction" among cooperating, competing or communicating brains is thus not measured directly, but inferred by independent observations aggregated by cognitive models and assumptions that link behavior and neural activation. This approach is clearly unsatisfactory if one wants to measure the neural substrates underlying the cooperation/deception between individuals that occurs simultaneously in time. To reveal the neural substrates supporting the development of the cooperation/deception between individuals, a direct observation of the "interaction" emerging between the brains of different subjects is necessary, and this could be obtained by measuring simultaneously their activity.

Recently, hemodynamic recordings of brain activity and their relative sophisticated analysis showed that it is possible to extract common characteristics shared by humans during the simultaneous observation of a movie (Hasson et al. 2004) or during the interaction in an "economic" transaction (Montague et al. 2002; King-Casas et al. 2005). Montague et al. called such simultaneous scanning of two people, using a functional magnetic resonance imaging (fMRI) device, "hyperscannings". In addition, the need for the adoption of different statistical tools was also suggested, for the analysis of fMRI hyperscanning recordings, which are different from the standard tools used in fMRI analysis. These new analysis tools have to take into account the fact that the data from fMRI hyperscannings arrives from different subjects scanned at the same time (Montague et al. 2002). In the past few decades, the measurement of the neuroelectrical cortical activity from non invasive scalp recordings has become a useful and consistent tool for the investigation of brain functions (Nunez 1995; Urbano et al. 1997, 1998; Babiloni et al. 2001, 2008; Astolfi et al. 2007a). Here, we show that it is possible to track the simultaneous activity of several human brains during cooperation/competition activity in a card game, by neuroelectrical hyperscannings through the use of different electroencephalographic devices (EEG hyperscannings). Furthermore, we illustrate a methodology for the estimation of functional connectivity values from the EEG data in different subjects that belong to the same team during the card game. This methodology uses the known concept of Granger causality (Granger 1969) but extends its applicability to the case of multi-subject analysis, which is necessary to analyze the data from the EEG hyperscannings. Such approach was suggested as a possible computational tool to be used in the EEG hyperscanning experiments., since it could complement the usual "one subject" analysis currently performed. Although the main aim of this work was related to the presentation of a suitable methodology to deal with EEG hyperscanning and their related functional connectivity estimations, we would like to demonstrate an application of the proposed set of techniques for the computation of the functional connectivity between estimated cortical signals computed from the EEG traces in a group of subjects playing a card game.

Methods

Experimental Design

Fourteen pairs of healthy subjects participated in the study. Informed consent was obtained from each subject after explanation of the study, which was approved by the local institutional ethics committee. The subjects were asked to play an Italian card game, called *tressette*. The game is played with two couples, with one couple sitting at north and south, and the other couple at east and west, like in the game of "Bridge". All the subjects studied were already able to play this game and understood the game rules well. The player to the dealer's left places the first card on the deck; the other players, in a clockwise order, play a card of the leading suit if they have one, otherwise a card of another suit. The round is won by the highest card of the suit. Ten cards were distributed and played for each game by every subject. Ten rounds represent an entire match. Ten matches were played between the two opposite couples. Each round took about 30–45 s, while each player was involved in making a decision for about 5–12 s. This is the time needed to generate a decision and make an overt verbal communication to the experimenter who was charged to move physically the card on the deck. Figure 1 presents a typical setup of the experiment performed. It is possible to observe the players and the cards to be placed on the desk disposed in front of them. The players are indicated by the signs N (North), E (East), S (South) and W (West). Team A is composed by the players N and S, while team B is composed by the player E and W. Two experimenters near the players during the EEG recording session were used to move the cards. Different markers were inserted in the recorded EEG files during the game development by an independent researcher, in order to make easier the successive data analysis. This was done in order to perform the analysis of EEG data related to particular time segments of the game. In particular, time information was inserted on the EEG data of each subject during the following moments in each round:

(1) the experimenter declares the round open (marker 1)
(2) the first player states the card to be moved by the experimenter (marker 2)

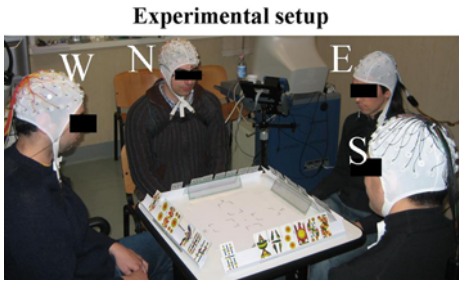

Fig. 1 EEG hyperscanning setup employed during a card game using several high resolution EEG devices. The card game was one of the most popular in Italy, called "tressette". The game is played with two pairs of subjects, those sitting at north (N) and south (S) against those set at west (W) and east (E). It is important to note that two experimenters seat during the game between N and W and between E and S in order to move on the deck the declared cards. Players do not move to play the card, only pronounced the card selected. The player to the dealer's left lays the first card on the deck; the other players, in a clockwise order, play a card, of the suit displayed, if they have one, otherwise of another suit. The round is won by the highest card of the suit

(3) the second player (of the opposite team) declares the card to be moved in opposition to the card of the first subject by another experimenter (marker 3)
(4) the third player (companion of the first one) states the card to be moved by the experimenter (marker 4)
(5) the fourth player (companion of the second one) states the card to be moved by the experimenter (marker 5)
(6) the experimenter declares the winner of the round and states the next player who starts the game (marker 6)

Figure 2 shows the time course of a typical round for this experiment. The T1, T2,…,T6 are the time instants in which the decisions and the relative markers were included in the EEG traces. The card pictures near the vertical lines are relative to the particular set of cards employed, typical for this game. The picture on the upper right part of the Fig. 2 presents again the setup employed and the experimenter that move the card on the deck after the subject's decision. In this study, we analyzed the EEG traces relative to the time interval between the first player's move (after the card was moved on the desk by the experimenter, marker T2) and after the overt verbalization of the card (marker T4). Videotape recordings of the entire sessions were also made in order to survey the correct behavior of the subjects during the game. Although the subjects were asked not to move muscles during each round and to minimize ocular movement, the presence of the EEG artefacts induced by the overt verbalization of the card to put on the desk was explicitly checked in the acquired traces. To this aim, electrodes were placed to monitor eye movements as well as to detect the occurrence of arm and/or head muscle artefacts on the players. Muscle movements were recorded through bipolar electrodes disposed on both

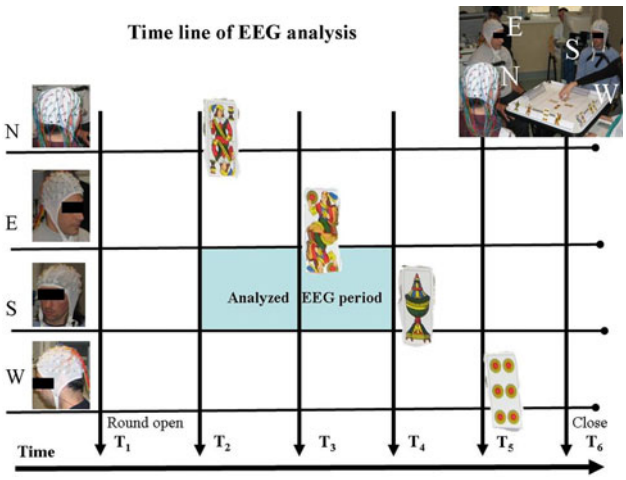

Fig. 2 Representation of the time course of the card game. On the bottom of the figure the time line of the experiment and the temporal markers (T1,…,T6) inserted during the evolution of the game. Figure represents a typical round of a card game, that lasts on average last 12–15 s. Each game consists of 10 rounds. The horizontal lines near the subject's heads are relative to the time course of the round for each particular subject. The time instant when the subject declares the card to be put on the deck is depicted by a vertical line, with a image beside. Such image is related to a particular card available to the player. The picture on the upper right part of the Fig. 2 presents an experimenter that move the card on the deck after the subject's decision of the card

m. biceps brachii and *m. triceps* sampled at 1 kHz. During the successive analysis, EEG readings due to ocular movements and muscular artefacts were removed using an independent component analysis (ICA) approach through a supervised procedure (Escudero et al. 2007). It is worth noting that the EEG traces are free of muscular artefacts induced by the overt verbalization of the player's decision. However, this particular choice of the analyzed time window has been generated here mainly for illustrative purposes of the possible advantage of the methodology proposed.

High Resolution EEG Hyperscannings in Normal Subjects

The neuroelectric hyperscannings were performed with four 64-channel, high resolution EEG devices, in a quiet large room where the subjects were comfortably seated. Such a room was tested previously for the absence of particular electrical noise. The EEG was recorded at 200 Hz, and anti-aliasing filtering was used in all the EEG devices. Electrode positions were digitized using 3D localization with respect to anatomic landmarks (nasion and two preauricular points) by using a Polhemius IsoTrack II magnetic device. To eliminate the sources of variance between the different EEG scanners, due to the electrical noise and the electrodes impedance, the same calibration signal was delivered in all the EEG devices, to adjust their

sensitivities before and after the execution of the EEG hyperscanning recordings, in order to equalize the different gains of the different acquisition devices.

Head-Brain Models

In order to estimate cortical activity from actual EEG scalp recordings, realistic-geometry head models reconstructed from T1-weighted structural magnetic resonance images (MRIs), collected with a Siemens 1.5T Vision Magnetom system, were employed. Subjects underwent these procedures and their MRIs were stored on a computer for successive analysis. Scalp, skull, and dura mater compartments were then segmented from the acquired MRIs and tessellated with about 5,000 surface triangles. A cortical source model was built using the following procedure: (i) the cortex compartment was segmented from the MRIs and tessellated to obtain a fine mesh with about 100,000 triangles; (ii) a coarser mesh was obtained by down-sampling the fine mesh to about 5,000 triangles (this was done by preserving the general features of the neocortical envelope, especially in correspondence of pre- and post-central gyri and frontal mesial area); (iii) an orthogonal equivalent current dipole was placed in each node of the tessellated cortical surface, with its direction parallel to the vector sum of the normals to the surrounding cortical surface triangles. Electrodes' positions were then aligned with the reconstructed scalp surface by using a nonlinear procedure for the fitting of their position by using fiducial points obtained on the scalp reconstruction (Urbano et al. 1998). In each subject each cortical nodes of the mesh were coded in the Tailarach coordinates, and then assigned to a proper Brodmann area, according to the public available atlas (Lancaster et al. 1997, 2000). It may be argued if a cortical head model could be adequate to model all the putative neural sources that could be involved in the generation of the recorded EEG data. Although the subcortical structures are not included in the employed source model, it has been pointed out how such subcortical structures barely could produce a recordable EEG data (Nunez 1995). This was mainly due to the distance of such subcortical structures from the scalp sensors as well as to the "closed field" potential they generate that was undetectable by such sensors (Nunez 1995).

Methods for EEG Hyperscannings

Estimation of Cortical Source Current Density from High Resolution EEG Measurement

High-resolution EEG technologies have been developed to enhance the poor spatial information content of the EEG activity (Urbano et al. 1998; Oliveri et al. 2003). In this work, cortical activity from EEG scalp recordings was estimated using a realistic head model. As described previously, this model consists of about 5,000 dipoles uniformly disposed on the cortical surface gathered from the MRI images, and the estimation of the current density strength for each dipole was obtained by solving the linear inverse problem according to techniques described in previous papers (Astolfi et al. 2007b; De Vico Fallani et al. 2007a) and illustrated in the following. The solution of the following linear system:

$$\mathrm{Ax} = \mathrm{b} + \mathrm{n} \tag{1}$$

provides an estimation of the dipole source configuration **x** that generates the measured EEG potential distribution **b**. The system also includes the measurement noise **n**, assumed to be normally distributed (Grave de Peralta Menendez and Gonzalez Andino 1999). **A** is the lead field matrix, where each j-th column describes the potential distribution generated on the scalp electrodes by the j-th unitary dipole. The current density solution vector $\boldsymbol{\xi}$ of Eq. 1 was obtained as (Grave de Peralta Menendez and Gonzalez Andino 1999; Babiloni et al. 2005):

$$\xi = \arg\min_{x}\left(\|\mathbf{A}x - b\|^2_{\mathbf{M}} + \lambda^2\|x\|^2_{\mathbf{N}}\right) \tag{2}$$

where **M**, **N** are the matrices associated to the metrics of the data and of the source space, respectively, λ is the regularization parameter and $\|x\|_M$ represents the M norm of the vector **x**. The solution of Eq. 2 is given by the inverse operator **G**:

$$\boldsymbol{\xi}(t) = \mathbf{G}\mathbf{b}(t), \quad \mathbf{G} = \mathbf{N}^{-1}\mathbf{A}'\left(\mathbf{A}\mathbf{N}^{-1}\mathbf{A}' + \lambda\mathbf{M}^{-1}\right)^{-1} \tag{3}$$

The optimal determination of the regularization term (λ) of this linear system was obtained by the L-curve approach (Hansen 1992; He et al. 2006). As a metric in the data space we used the identity matrix, while as a norm in the source space we used the following metric:

$$\left(\mathbf{N}^{-1}\right)_{ii} = \|\mathbf{A}_{\cdot i}\|^{-2} \tag{4}$$

where $(\mathbf{N}^{-1})_{ii}$ is the i-th element of the inverse of the diagonal matrix **N** and all the other matrix elements N_{ij} are set to 0. The L_2 norm of the i-th column of the lead field matrix **A** is denoted by $\|\mathbf{A}_{\cdot i}\|$.

Using the relations described above, an estimate of the signed magnitude of the dipolar moment for each cortical dipoles was obtained for each time point. As the orientation of the dipole was defined to be perpendicular to the local cortical surface in the head model, the estimation process returned a scalar rather than a vector field. The spatial average of the signed magnitude, of all the dipoles belonging to a particular ROI at each time sample, was used to estimate the waveforms of cortical ROI activity in that ROI, indicated as $\boldsymbol{\rho}(t)$ to highlight their time-

dependence. Spatial averaging can be expressed in terms of matrix multiplication by a matrix **T.** This matrix is sparse and has as many rows as ROIs, and as many columns as the number of dipole sources. ROI cortical current density waveforms can then be expressed as:

$$\boldsymbol{\rho}(t), = \mathbf{Tx}(t) = \mathbf{TGb}(t) = \mathbf{G}_{\mathrm{ROI}}\mathbf{b}(t), \quad \mathbf{G}_{\mathrm{ROI}} = \mathbf{TG} \qquad (5)$$

where $\mathbf{b}(t)$ is the array of the waveforms recorded from the scalp electrodes and $\mathbf{x}(t)$ is the array of the cortical current density waveforms estimated at the cortical surface. The $\mathbf{G}_{\mathrm{ROI}}$ matrix only depends on geometrical factors, and can thus be computed and stored off-line. The matrix multiplication can be interpreted as a spatial filtering of the scalp potenital $\mathbf{b}(t)$, using the elements of $\mathbf{G}_{\mathrm{ROI}}$ as weights. In this way, we could obtain time-varying waveforms at the level of different cortical areas. In the next paragraph we describe such cortical areas as coincident with the particular Brodmann areas for all the subjects involved in the present study.

Generation of the Regions of Interest (ROIs)

Cortical regions of interest (ROIs) were drawn on the computer-based reconstruction of the individual cortical surface of each subject. Such ROIs were segmented automatically on the basis of their Talairach coordinates and of the anatomical landmarks available. The ROIs considered in this study were those suggested by the previous literature, which are involved in the mechanism of the "decision-making" processes, then involving dorsolateral prefrontal cortical (DLPFC) and parietal regions, as well as the cingulate cortices (Anterior Cingulate Cortex; ACC and the Cingulate Motor Area; CMA). Also, the primary and supplementary motor areas were selected since the subject could have the intention to move the card, although this was forbidden by the task instruction. ROIs representing the left and right primary motor areas (MI) included Brodmann area 4 (BA 4). ROIs representing the Supplementary Motor Area (SMA) were obtained from cortical voxels belonging to the more general BA 6. ROIs from the right and left parietal areas including BA 7 and 5 were also selected. The DLPFC regions including the BAs 8, 9/46 and 10 were then selected, together with the Anterior Cingulate Cortex (ACC) defined by comprising the BAs 24, 25 and 33. Finally, the Cingulate Motor Area (CMA) on both sides was also segmented and employed in the present study. It may be argued whether the brain activity in ROIs not so close to the electrode array placed on the scalp surface could be estimated with few errors. Previous simulation studies assessed that errors in the estimation of cortical activity and connectivity, by using the presented approach, are below the 5% if there is a sufficient signal to noise ratio (at least 3), and a sufficient time length of the EEG recordings (15 s or more, Babiloni et al. 2005; Astolfi et al. 2005). Both the conditions were met in this study. In fact, as explained above, the different trials for the game were linked together to return a time series to be analyzed that exceed 15 s in all the recordings performed. We computed the signal-to-noise ratio (SNR) of the EEG data by using the estimator provided by Raz and coworkers (Raz et al. 1988). Previous simulation studies on the performances of the Granger-causality estimators suggested that also in favourable conditions of SNR and signal length there is an upper limit on the number of ROIs to be employed, to get reconstruction errors below 5% (Astolfi et al. 2005). For this reason, in the current condition a limited number of ROIs (14) have been selected from the entire set of Brodmann areas available.

Multivariate Methods for the Estimation of Connectivity: The Estimation of Partial Directed Coherence (PDC)

Many EEG and/or magnetoencephalography (MEG) frequency-based methods that have been proposed in recent years, for the assessment of the directional influence of one signal on another are based mainly on the Granger (1969) theory of causality. Granger theory mathematically defines what is a "causal" relation between two signals. According to this theory, an observed time series x(n) is said to cause another time series y(n) if the knowledge of x(n)'s past significantly improves prediction of y(n). This relation between time series is not necessarily reciprocal; x(n) may cause y(n) without y(n) causing x(n). This lack of reciprocity allows the evaluation of the direction of information flow between elements (Kaminski and Blinowska 1991; Kaminski et al. 2001). Partial Directed Coherence (PDC) is a particular estimator of the Granger causality in the frequency domain, introduced in the last years by Baccalà and Sameshima (Baccalà and Sameshima 2001). In the following, a brief explanation of the PDC estimation procedure is provided. Let Y be a set of cortical waveforms, obtained from several cortical regions of interest (ROI) as described above:

$$\mathrm{Y} = [\mathrm{y}_1(\mathrm{t}),\ \mathrm{y}_2(\mathrm{t}), \ldots,\ \mathrm{y}_\mathrm{N}(\mathrm{t})]^\mathrm{T} \qquad (6)$$

where t refers to time and *N* is the number of cortical areas considered.

Multivariate autoregressive process (MVAR) are largely used in the modeling of EEG time series. In fact, they provided the required processing steps to derive parameters to be used in the arsenal of methods employed to assess functional connectivity between the EEG time-series (reviewed in Schlögl and Supp 2006). In the following, in agreement with previous literature, we used a MVAR process as an adequate description of the data set Y as follows:

$$\sum_{k=0}^{p} \Lambda(k) Y(t-k) = E(t) \qquad \text{with } \Lambda(0) = \mathrm{I} \tag{7}$$

where $\mathbf{E}(t) = [e_1(t),\ldots,e_N]^T$ is a vector of multivariate zero-mean uncorrelated waveforms representing a collection of white noise signals, $\Lambda(1)$, $\Lambda(2),\ldots,\Lambda(p)$ are the $N \times N$ matrices of model coefficients and p is the model order. In the present study, p was chosen by means of the Akaike Information Criteria (AIC) for MVAR processes. It has been noted that, although the sensitivity of MVAR performance depends on the model order, small model order changes do not influence results (Grave de Peralta Menendez and Gonzalez Andino 1999).

A modified procedure for the fitting of MVAR on multiple trials was adopted (Babiloni et al. 2005; Astolfi et al. 2008; Grave de Peralta Menendez and Gonzalez Andino 1999; Ding et al. 2000). When many realizations of the same stochastic process are available, as in the case of several trials of an event-related potential (ERP) recording, the information from all the trials can be concatenated to increase the reliability and statistical significance of the model parameters. Once an MVAR model is adequately estimated, it becomes the basis for subsequent spectral analysis. To investigate the spectral properties of the examined process, Eq. 7 is transformed to the frequency domain:

$$\Lambda(f)\mathbf{Y}(f) = \mathbf{E}(f) \tag{8}$$

where

$$\Lambda(f) = \sum_{k=0}^{p} \Lambda(k) e^{-j2\pi f \Delta t k} \tag{9}$$

and Δt is the temporal interval between two samples.

It is then possible to define *partial directed coherence* as:

$$\pi_{ij}(f) = \frac{\Lambda_{ij}(f)}{\sqrt{\sum_{k=1}^{N} \Lambda_{ki}(f)\Lambda_{kj}^{*}(f)}} \tag{10}$$

which bears its name by its relation to the well-known concept of partial coherence (Bendat and Piersol 1993). The PDC from j to i, $\pi_{ij}(f)$, describes the directional flow of information from the ROI activity $s_j(n)$ to $s_i(n)$, where upon common effects produced by other ROIs $s_k(n)$ on the latter are subtracted leaving only a description that is exclusive from $s_j(n)$ to $s_i(n)$.

PDC values are in the interval [0,1] and the normalization condition

$$\sum_{n=1}^{N} \left|\pi_{ni}(f)\right|^2 = 1 \tag{11}$$

is verified. According to this condition, $\pi_{ij}(f)$ represents the fraction of the time evolution of ROI j directed to ROI i, as compared to all of j's interactions to other ROIs. The application of the PDC connectivity methods to the ROIs waveforms returns a cortical network for each frequency band of interest: (θ 4–7 Hz, α 8–12 Hz, β 13–29 Hz, γ 30–40 Hz).

Statistical Evaluation of Functional Connectivity Measurements Within a Single Subject: The Estimation of the Null Distribution

As PDC functions have a highly nonlinear relation to the time series data from which they are derived, the distribution of their estimators is not well established, although a recent attempt has been made in this direction (Sato et al. 2009). This makes tests of significance difficult to perform. A possible solution to this problem was proposed by Kaminski et al. (2001) and consists of the use of a surrogate data technique (Theiler et al. 1992), in which one generates an empirical distribution for a given estimator when interactions between signals are removed. Significance tests based on this empirical distribution can then be performed. Specifically, one randomly and independently shuffles the time series data from each ROI to create a surrogate data set. A bivariate autoregressive model is then fit to the shuffled data and the PDC functions are computed from such a model. Carrying out this process many times, each time performed on an independently shuffled data set, it is possible to construct an empirical distribution for the PDC functions. Using this distribution, one can then assess the significance of the causal measures evaluated from the actual data. Without having an explicit formulation for the shape of this distribution, one can thus compute an empirical threshold for a given significance level. The shuffling procedure was performed for a sufficient number of times to reach the statistical significance level set to 0.001%, Only the estimated PDC connections that are statistically significant (at $P < 0.001$, Bonferroni corrected for multiple comparisons), after the comparison with the surrogate distribution of the PDC values on the same ROIs obtained with this Montecarlo-like procedure (Astolfi et al. 2005), were considered for the analysis. This procedure allows us to consider only the particular functional links that are not due to chance and that are different, in a consistent way, from the background EEG. It must be noted that an alternative solutions for the estimation of a probability distribution for the PDC could be also to fit the obtained empirical distribution with a reduced number of computations to a already know one, such a β distribution for instance. Such a distribution can then be adapted easily with a small number of bootstrap realizations of the PDC.

Statistical Evaluation of Functional Connectivity Measurements in Multiple Subjects

One particular assumption of the MVAR methods, used for the estimate of the causality relationships between different waveforms, is the same "noise" characteristic for each MVAR model used for the simultaneous estimation of the coefficient from the different waveforms recorded. However, due to the fact that the EEG of the different subjects could show large deviations from subject to subject, a normalization procedure is needed for the estimation of causality between the multi-subject MVAR. In this respect the statistical treatment of each subject is related to the use of a z-transformation before entering the waveforms inside the general MVAR model, for the relation of the causality relationships between the group. The z-score transformation was first applied to the data of each subject, by taking into account the level of the noise originated in each dataset, and then the MVAR procedure was applied to the two set of data related to the two subjects. The estimation of the level of noise in each individual dataset was generated by using the EEG during the resting state before the start of each trial of the card game. It is worth of note that a similar procedure was suggested to improve also the estimation of connectivity from local field potentials and spikes measurements by using the generalized PDC (Taxidis et al. 2010).

Generation of the Null Distribution for the Functional Connectivity Estimates Between Subjects

The implementation of these methods, to compute the functional connectivity between cortical EEG signals estimated in different subjects, has been performed by generating a unique MVAR model based on the EEG data from two subjects belonging to the same team (i.e., in this case, the first and the second player of a team). From this set of EEG hyperscannings, we generated surrogate data in order to build a probability distribution related to random connectivity, and to generate thresholds of statistical significance at $P < 0.001$, Bonferroni corrected for multiple comparisons. Then, the functional connectivities between the cortical signals estimated in the brains of the two players were computed and plotted if they exceeded the thresholds obtained by chance. We applied PDC algorithms for the analysis of functional connectivity patterns within each brain, as well as for the functional connectivity between the cortical EEG signals estimated in different subjects, on the z-transformed estimated cortical waveforms.

Statistical Validation of the Functional Connectivities Estimated Between Players of the Same Team

From all that has been described above, it is then possible to estimate the functional connectivity by PDC between signals estimated from different cortical areas of two subjects. However, the estimation of the functional connectivity could not only be performed within the EEG signals estimated from members of the same team, but also between signals estimated in members of the two different teams seated at the same table. This evaluation could clarify if such functional connectivity also exists during the game *between players belonging to the two different teams*. If so, such functional connectivity could be related to confound factors affecting all the players during the game, irrespective to their team belonging. For this reason, we computed the null distributions and estimated the statistical significant functional connectivity not only for the signals estimated in members of a same team but also between signals estimated in members of the two different teams. Statistical significance of the functional connectivity between signals estimated in different subjects were assessed at the $P < 0.001$, Bonferroni corrected for the multiple comparisons. In this way, we generated the randomization of the players, with respect to the variable "team" for all the players that participated in the same card game. No attempt to generalize this randomization across the different "tables" or game sessions was performed.

Graph Analysis

The application of the functional connectivity methods by PDC on EEG data returns a pattern of statistically significant links between cortical areas (Astolfi et al. 2007a). However, since the resulting connectivity patterns could have a relatively large size and a complex structure, the interpretation of these functional networks remains an open issue. For this reason, there is a diffuse interest in the development and validation of mathematical tools to extract relevant features from the estimated complex cerebral networks (Varela et al. 2001; Tononi et al. 1994; Sporns 2006). Since a graph is a mathematical representation of a network, which is essentially a list of nodes and a list of the connections between them, a way to characterize the topological properties of the estimated or measured cerebral networks was addressed using a theoretical graph approach (Sporns 2006). A weighted graph, is a graph where the arcs between the nodes have an associated value for them. In this similarity, a weighted graph represents a pattern of connectivity if the nodes are the ROIs considered and the weighted arcs, between nodes, are the estimated functional connections between ROIs obtained

by applying the PDC on the cortical data. It is then possible to apply tools already validated and derived from the graph theory to the estimated connectivity graphs during the task performance. Subsequently, the following conventions are followed: the graph is described by N nodes (equal to the number of the ROIs considered here), each arc of the graph from the i-th node toward the j-th node will be labeled with the intensity of the PDC value and will be described as wij. The N × N matrix of the weights between all the nodes of the graph is the connection matrix W. In particular, we would like to use the indices related to the strength of the estimated functional links between the cortical areas, to characterize the behavior of the estimated network during the time window occurring between the placing of the card by the first subject and the overt verbalization related to the card selection of their companion. Such indices will be described in the following. The simpler attribute for a graph's node is its degree of connectivity, which is the total number of connections with other points. In a weighted graph, the natural generalization of the degree of a node i is the node strength or node weight (Yook et al. 2001). This quantity has to be split into in-strength **S-in** (indegree) and out-strength **S-out** (outdegree) indices, when directed relationships are being considered, as in the present case with the use of the PDC values (De Vico Fallani et al. 2007b).

$$\text{S-in}(i) = \Sigma j \; wij \; j \;\; = 1, \ldots, N \tag{12}$$

S-in(i) represents then the amount of all the incoming arcs from the graph toward the node i-th, and is a measure of the inflow of the graph toward such a node. A similar measure can be derived for the outflow from the i-th node of the graph, according to the following formula where the same conventions for 1) holds:

$$\text{S-out}(i) = \Sigma j \; wji \tag{13}$$

Note that in this case the sum is upon all the outgoing weighted arcs that move from the i-th node towards all the other nodes of the graph.

Statistical Analysis

The estimated values of the S-in and S-out indices were then subjected to a separate analysis of variance (ANOVA) in the different frequency bands, using as main factor the ROIs employed (factor ROI) and the player involved (factor PLAYER). The Duncan post-hoc test, performed at the 5% level of significance was also used (Zar 1984).

Results

As described in the "Methods" section, we gathered EEG hyperscanning data obtained during the execution of a card game, in which four subjects belonging to two competing teams were involved. (details in "Methods" section). In particular, in each pair of players belonging to the same team we identified the first player and the second player. The first player declares the card to be moved on the deck (that the experimenter physically put there), while the second player has to support the move by declaring the card that maximizes the score for the couple, in order to defeat the opposing couple. Subtle movements of the subject's arms were detected by using EMG signals.

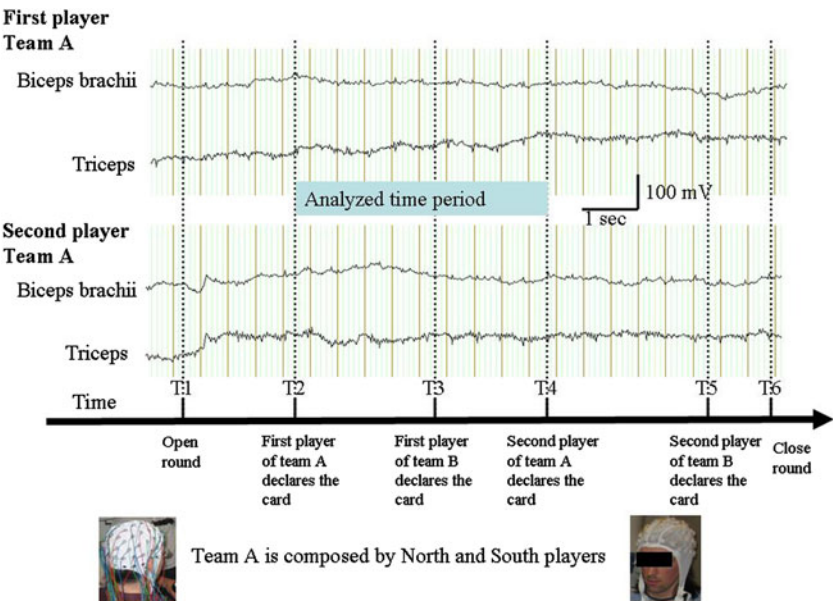

Fig. 3 The Figure shows the EMG traces gathered in a couple of players belonging to the same team during a round of the card game. The EMG traces are relative to the North player (upper part of the Figure) for muscles biceps brachii and triceps. The same was shown in the lower panel for the player South (S). The time line on the bottom showed the different events and the triggers inserted in the EEG traces during the evolution of the game. The meaning of the triggers T1,…,T6 are described by the legends therein

Figure 3 presents a series of EMG signals collected from a representative couple of players that belong to the same team. The EMG traces are relative to a complete round of the game, i.e., from marker 1 to the marker 6 of the sequence already described in the "Methods" section. It is possible to observe as the muscles employed are relatively silent during the performance of the trial.

The brain activity estimates, in all the cortical ROIs considered for each of the first players in all the groups analyzed, were then subjected to the functional connectivity analysis via the use of PDC (Baccalà and Sameshima 2001). Only the statistical significant functional connectivity patterns, as estimated against the surrogate distribution with a significance level of $P < 0.001$ (Bonferroni corrected for the multiple comparisons) were then considered for further analysis. The statistically significant functional connectivity patterns were then summarized as total outflow by summing the intensities of the statistically significant connectivity from each specified cortical area with all the signals estimated in the ROIs of the same subject. This measurement highlights which ROIs presents an estimated cortical signals that are causally-related with the cortical signals estimated in other parts of the cortex; this measure is known in graph theory as outdegree (S-out; Sporns 2006). It is also possible to compute the total amount of the functional connectivity intensities for the signals estimated from all the other cortical areas towards each particular considered ROI. Such a measure is called indegree (S-in; Sporns 2006). Thus, Fig. 4 presents the average values for the outdegrees and the indegrees for all the considered ROIs for a group of subjects when they acted as first player (i.e., the player that performs the first card move) in the θ and α frequency bands, while Fig. 5 presents the same information for the β and γ frequency bands.

It is possible to observe large outdegree values for the signals estimated in the ROIs modeling the cingulate motor area (CMA), the anterior cingulate cortex (ACC) and the prefrontal areas described by the Brodmann area 8. The average profile of the indegree and outdegree graphs is

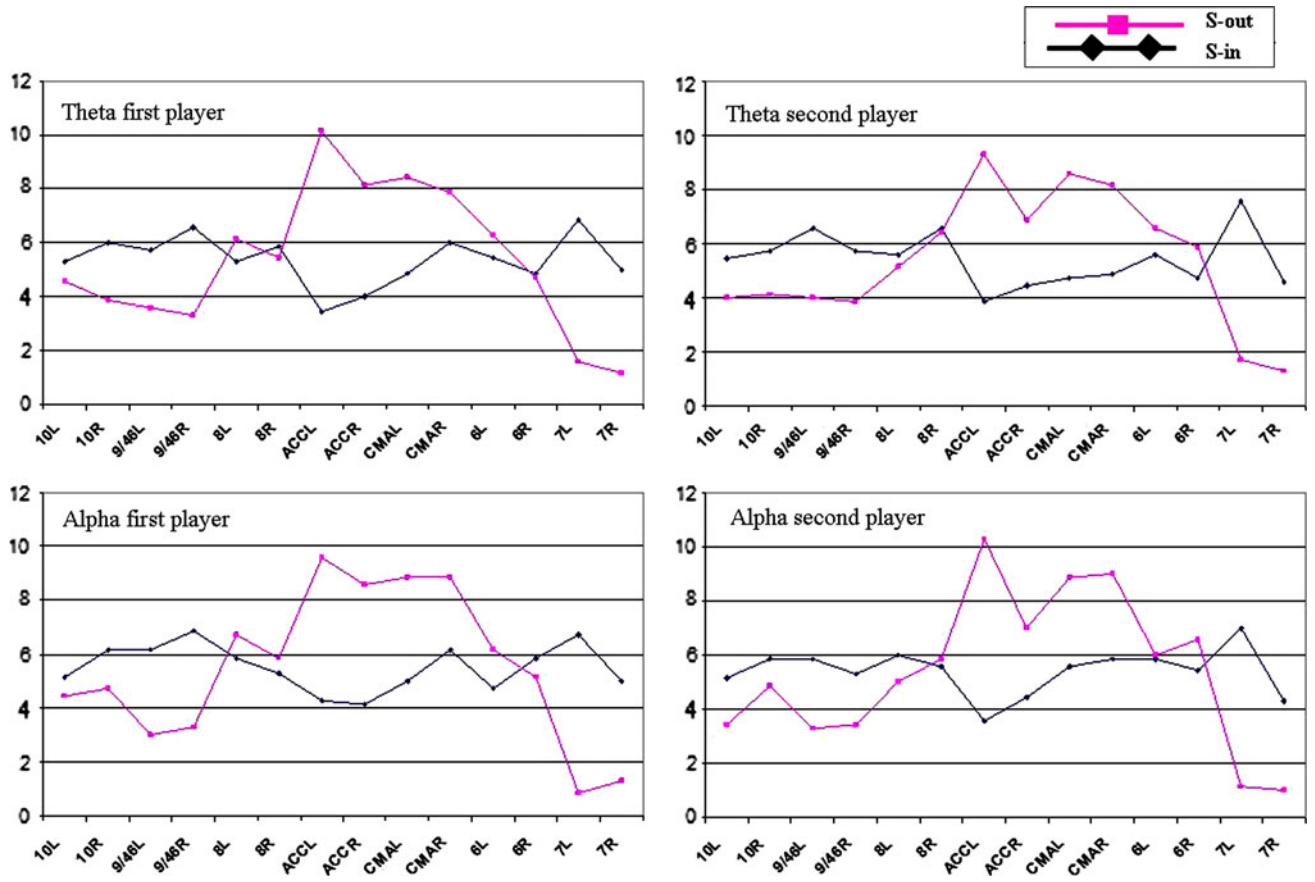

Fig. 4 Average graph of the indegrees (dark line) and outdegrees (light line) for the different ROIs considered in this study. The data presented is related to the θ (first row) and α (second row) frequency bands. The first row presents the indegree and outdegree average data from all the subjects that act as first player (left) and second player (right) in each couple examined for the θ frequency. The second row presents the same data for the α frequency bands. The ROIs are related to the Brodmann Areas depicted on each individual cortical surface. On the *x*-axes are the name of the ROI considered, with the postfix L for left and R for right hemisphere, respectively. The y axes shows the average number of functional connections that arrive (dark lines) or depart (light lines) from the considered ROIs

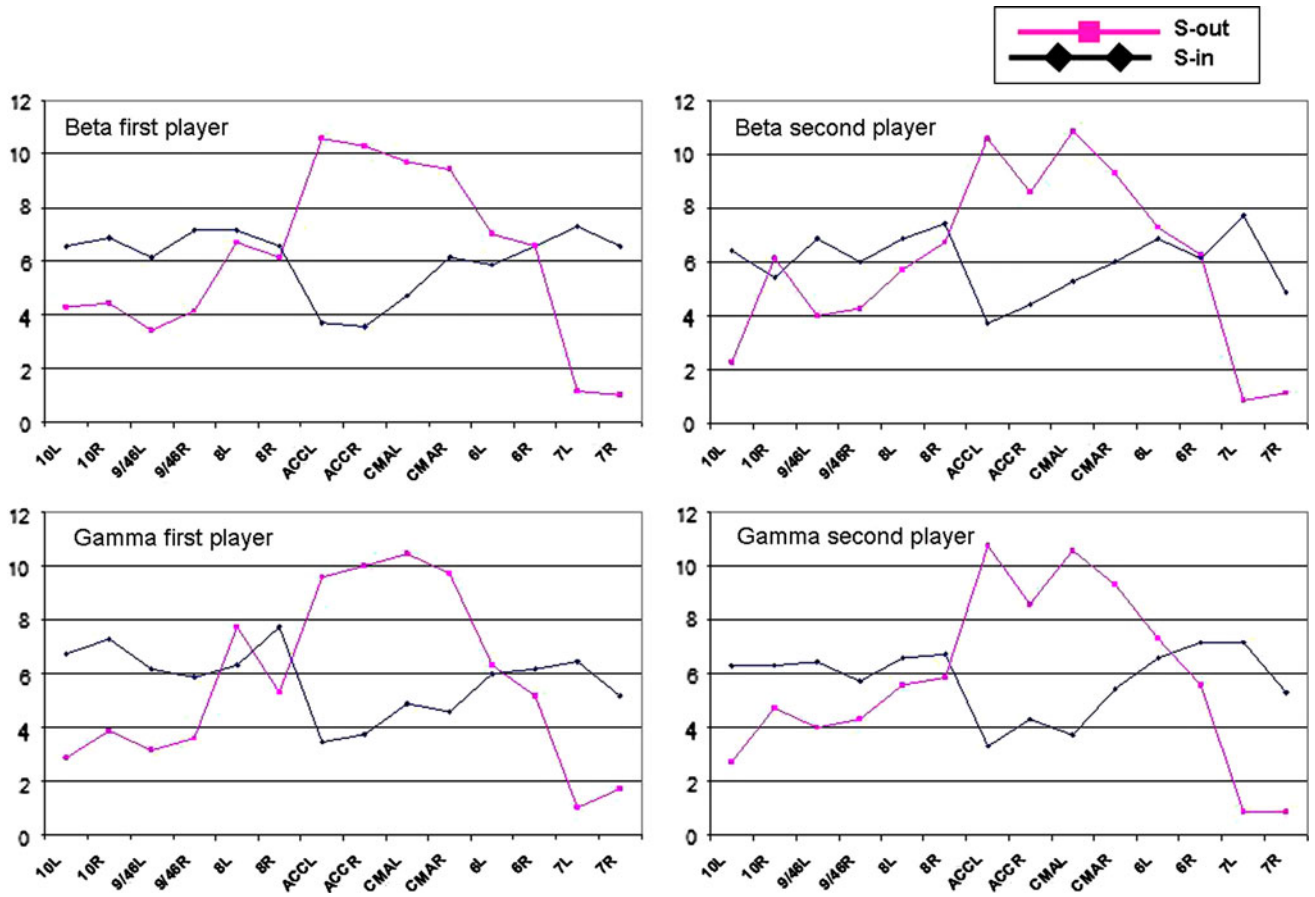

Fig. 5 Average graph of the indegrees (dark line) and outdegrees (light line) for the different ROIs considered in this study. The data presented is related to the β (first row) and γ (second row) frequency bands. The first row presents the indegree and outdegree average data from all the subjects that acts as first player (left) and second player (right) in each couple examined for the β frequency. The second row presents the same data for the γ frequency bands. Same conventions as in the previous figure

somewhat similar between the two players, although statistically significant differences (at $P < 0.001$) are present, as described in the following sections.

S-in Analysis

The ANOVA performed on all the frequency bands reported the statistical significant interactions between the main factors ROI and PLAYER, as well as the significance of the main factor ROI. In the case of ROI × PLAYER interactions, we have in the different frequency bands $F = 3.96$ for θ, $F = 3.79$ for α, $F = 5.65$ for β, and $F = 4.03$ for γ bands, respectively. All these values resulted in a statistical significance of $P < 0.0001$ at minimum. Post-hoc tests return a list of differences between the S-in index across the two players with a minimum significance of $P < 0.001$ as described in the following. In the θ band, statistical significant differences were found for the signals estimated in cortical areas including Brodmann areas 9/46L, 9/46R, 8R, CMAR, 7L. In the α band, differences were found for the signals estimated in the following cortical areas 9/46R, ACCL, 6L, while in the β band such differences were found in the areas A10R, 9/46R, ACCR, 6L, 7R. Finally, in the γ band the significant differences were found between the signals estimated in the cortical areas 10R, 8R, CMAL, CMAR, 6R.

S-out Analysis

The ANOVAs performed on all the frequency bands always reported the statistically significant interaction between the main factors ROI and PLAYER, as well as the significance of the factor ROI. In the case of ROI × PLAYER, we have $F = 2.26$ for θ, $F = 3.59$ for α, $F = 5.6$ for β, and $F = 4.92$ for γ frequency bands. All these values result in a statistical significance of $P < 0.0001$ at least. Post-hoc tests return the following differences in the S-out index across the two players, with a minimum statistical significance of $P < 0.0001$. In the θ band, differences were found in the index computed from the signals estimated in the ACCR and 6R cortical areas while in the α band differences were found for the index

computed on signals estimated in areas 10L, 8L, ACCR, 6R. In the β band, we found statistical differences for the index computed on signals estimated in the 10L, 10R, 8L, ACCR, CMAL cortical areas, while in the γ band such differences were found in the areas 8L, ACCR, ACCL and 6L.

Estimation of the Functional Connectivity Between Signals Estimated in Cortical Areas of Different Subjects

In agreement with the procedure described above, the estimation of the functional connectivity between the signals estimated in the cortical areas of different subjects has been performed for all the possible pairs of subjects that participated in the same game session. Results suggested that only the players that belonged to the same team across the different tables showed statistically significant functional connectivity between the signals estimated from different cortical areas, at the chosen level of statistical significance ($P < 0.001$ Bonferroni corrected for multiple comparisons). In fact, the estimated functional connectivity between estimated cortical signals in subjects that did not belong to the same team did not reach the statistical threshold for significance in all the couples analyzed. The statistical values obtained were rather low when compared to the average level of the null distributions evaluated, and very sporadic links (six in total in all the couple analyzed) appeared in the different frequency bands between such couples. In particular, two links appeared in the θ frequency band in a single couple of subjects and four links appeared in the γ band in another single couple of subjects (different from the previous one). However, these few significant links in two subjects are not sufficient to generate any valid conclusion for the analyzed population. On the contrary, the estimated functional connectivity between estimated cortical signals in subjects that belong to the same team was rather strong and present in the α, β and γ frequency bands analyzed, while it was absent in the θ band. In particular, Fig. 6 presents the statistically significant functional connectivity by PDC between estimated cortical signals that are in common across all the pairs of players considered in this experiment in the β and γ bands. This means that the represented functional links between the signals estimated from different cortical areas in different subjects are present in all the couples analyzed, that belong to the same team.

The arrows in Fig. 6 coded the direction of the Granger causality between the signals estimated in a couple of cortical areas. In addition, the color of the connection returning the information on the number of couple in which such connectivity was active. For instance, if a functional connectivity link is depicted in yellow, this means that such link is present in all the couples analyzed; if a functional connectivity is instead depicted in orange it means that such link was present in all the couples but one. It is interesting to note how those functional links are directional, as resulted from the properties of the employed PDC estimator. Such functional connectivity causally put in connection the signals estimated from the ROIs of the first player with the signals estimated in the ROIs of the second player. We also observed functional connectivity links that

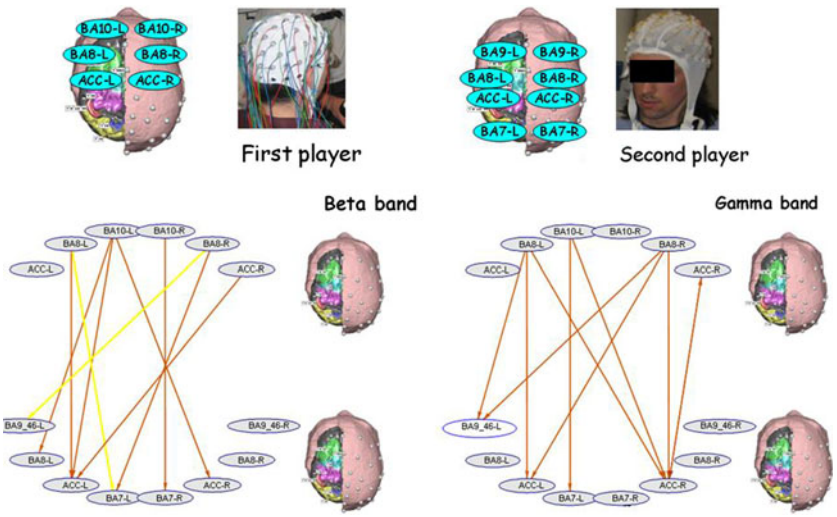

Fig. 6 Representation of the functional connectivity obtained for all the teams analyzed in the present experiment. The arrows depict functional connectivity between different ROIs in the two sets of players. Yellow arrows depict the functional links that are statistically significant in all the pairs of players investigated, while the orange arrows depict functional links that are statistically significant in all the couples but one. The time interval between the first player's move and the response of their companion (i.e., the "second player") was analyzed with EEG hyperscanning

suggest a causal relation between the signals estimated from the prefrontal areas 8 and 9/46 of the first player and the signals estimated mainly in the anterior cingulate cortex and the parietal areas of the second player.

Discussion

Methodological Considerations

We presented a methodology for the gathering of the EEG activity in several subjects simultaneously (EEG hyperscanning). In addition, we proposed the use of a modified functional connectivity estimator to assess Granger-causal relationships between the signals estimated in ROIs of different subjects. Here, we would like to briefly discuss some methodological aspects of this approach, in order to made clear the actual limitations of the technology employed both in the experimental design and in the use of the signal processing methodology.

In the experimental design adopted, due to the nature of the complex "naturalistic" task chosen, we cannot differentiate between the EEG signals related to the decision of the card to be chosen by the second player and the EEG related to the verbalization of such decision (i.e., between the trigger 2 and 4). This fact has to take into account in the discussion of the results obtained.

The functional connectivity computed in this study expressed statistical and mathematical properties of the estimated cortical time series in the analyzed population. However, it is largely debated how this functional connectivity estimates is linked to the real cortical connectivity occurring in the brain. This operative limitation is not related to the particular methodology here employed (i.e., PDC) but is rather extended to the several methods already available and used in neuroscience literature, such as Directed Transfer Function (DTF), spectral coherence, Mutual Information (MI), Phase lag synchrony (PLS), Structural Equation Modeling (SEM) or Dynamic Causal Modeling (DCM). In fact, the equivalence between the estimation of functional connectivity and the behaviour of the underlying neural systems have to be adopted with extreme caution (Horwitz 2003; Stephan et al. 2008).

Here, an extension of the hyperscanning methodology already provided by using hemodynamic signals (Montague et al. 2002; Hasson et al. 2004; King-Casas et al. 2005;) is performed by using neuroelectric signals of brain activity. The presented methodology could be useful for the evaluation of the cerebral activity of a group of subjects that interacts one to each other. It must be understood that the functional connectivity estimation is the computation of a mathematical entity (based on the definition of the Granger-causality, Granger 1969; Formisano et al. 2004) that obviously does not describe a "passage" of some physical quantity between two brains, but rather describes the statistical and mathematical properties of signals estimated from different cortical areas of the subjects.

Experimental Considerations

As already described, the use of hemodynamic hyperscanning was suggested in 2002 (Montague et al. 2002), and a clear demonstration of the potential of this approach has been produced recently (Hasson et al. 2004; King-Casas et al. 2005). In the approach presented here, we employed a technique that it is able to gather the brain activity and to compute the functional connectivity from the estimated cortical signals in groups of four subjects, during face-to-face interactions, with a remarkable time-resolution and an appreciable spatial resolution.

The particular results, presented here for illustrative purposes only, are obtained with the application of the described methods to the EEG hyperscannings of card players during a cooperative game. In summary, such results show that the signals estimated in the anterior cingulate cortex (ACC) of the second players of the team shown a statistically significant Granger-causality with the signals estimated in different cortical areas of the first players of the same team. Moreover, in the first players of the analyzed teams, the signals estimated from the prefrontal areas (BA8) on both brain hemispheres develop a statistically significant Granger-causality with the signals estimated in the several regions of the brain of their companions (ACC, BA7).

Card games tasks were employed in literature to monitor the brain structures involved in the evaluation of uncertainty and risks (Preuschoff et al. 2006). It has been found that the altered risk sensitivity and gambling in humans suggest that orbitofrontal cortex (modelled in this paper by BA10) is involved in evaluation of the uncertainty of outcomes (Bechara et al. 2000; Hsu et al. 2005; Sanfey et al. 2003). ACC has been found also active with decisions related to conflicts during financial risk-taking (Kuhnen and Knutson 2005), while medial prefrontal cortex activity has been observed to correlate in gambling with specific combination of expected reward and risks that elicit activation of structures such a striatal areas and insula (Tobler et al. 2005).

The presented results, obtained in all the teams investigated, are fully consistent with previous studies on isolated brains, that indicated the ACC as the cortical site in which humans represent the other's intentions in the brain (Knobe 2005). In particular, several lines of evidence have suggested the role of the ACC in effort-related decision making, including ERP investigations (Mulert et al. 2005), or lesion studies in animals (Walton et al. 2002). Moreover,

it has been proposed that ACC activity might reflect the amount of effort associated with cognitive processing in, for example, conflict monitoring (Botvinick et al. 2004). Therefore, the concept of mental effort might be a promising candidate for the understanding of ACC activity during different cognitive processes, such as conflict monitoring or reward-based action selection.

Conclusions

The obtained results suggest that the EEG hyperscanning, together with the methodology for the estimation of the functional connectivity between different subjects could be used in the experimental situations in which the collection of simultaneous subject's activity is of interest. The estimation of functional connectivity has several limitations in its application in neuroscience. Apart the technical issues, discussed previously, the main issue here is the capability of such mathematical properties of the gathered EEG signals to reflect intrinsic cortical connectivity properties of the underlying neural tissue. Although some simulations suggested that this is the case (Astolfi et al. 2005, 2007a) the equivalence between estimated "functional" connectivity and "real" cortical connectivity have to be taken with caution.

Acknowledgments This study was performed with the support of the COST EU project NEUROMATH (BM 0601).

References

Astolfi L, Cincotti F, Mattia D, Babiloni C, Carducci F, Basilisco A et al (2005) Assessing cortical functional connectivity by linear inverse estimation and directed transfer function: simulations and application to real data. Clin Neurophysiol 116(4):920–932

Astolfi L, Cincotti F, Mattia D, Marciani MG, Baccala L, de Vico Fallani F et al (2007a) Comparison of different cortical connectivity estimators for high-resolution EEG recordings. Hum Brain Mapp 28(2):143–157

Astolfi L, de Vico Fallani F, Cincotti F, Mattia D, Marciani MG, Bufalari S et al (2007b) Imaging functional brain connectivity patterns from high-resolution EEG and fMRI via graph theory. Psychophysology 44(6):880–893

Astolfi L, Cincotti F, Mattia D, de Vico Fallani F, Tocci A, Colosimo A et al (2008) Tracking the time-varying cortical connectivity patterns by adaptive multivariate estimators. IEEE Trans Biomed Eng 55(3):902–913

Babiloni C, Babiloni F, Carducci F, Cincotti F, Rosciarelli F, Rossini PM et al (2001) Mapping of early and late human somatosensory evoked brain potentials to phasic galvanic painful stimulation. Hum Brain Mapp 12(3):168–179

Babiloni F, Cincotti F, Babiloni C, Carducci F, Mattia D, Astolfi L et al (2005) Estimation of the cortical functional connectivity with the multimodal integration of high resolution EEG and fMRI data by Directed Transfer Function. Neuroimage 24(1):118–131

Baccalà LA, Sameshima K (2001) Partial directed coherence: a new concept in neural structure determination. Biol Cybern 84:463–474

Bechara A, Damasio H, Damasio AR (2000) Emotion, decision-making and the orbitofrontal cortex. Cereb Cortex 10:295–307

Bendat JS, Piersol AG (1993) Engineering applications of correlation and spectral analysis. Wiley, New York

Botvinick M, Cohen JD, Carter CS (2004) Conflict monitoring and anterior ingulate cortex: an update. Trends Cogn Sci 8:539–546

De Vico Fallani F, Astolfi L, Cincotti F, Mattia D, Tocci A, Marciani MG et al (2007a) Extracting information from cortical connectivity patterns estimated from high resolution EEG recordings: a theoretical graph approach. Brain Topogr 19(3):125–136

De Vico Fallani F, Astolfi L, Cincotti F, Mattia D, Marciani MG, Salinari S et al (2007b) Cortical functional connectivity networks in normal and spinal cord injured patients: evaluation by graph analysis. Hum Brain Mapp 28(12):1334–1346

Ding M, Bressler SL, Yang W, Liang Ding H (2000) Short-window spectral analysis of cortical event-related potentials by adaptive multivariate autoregressive modeling: data preprocessing, model validation, and variability assessment. Biol Cybern 83:35–45

Escudero J, Hornero R, Abásolo D, Fernández A, López-Coronado M (2007) Artifact removal in magnetoencephalogram background activity with independent component analysis. IEEE Trans Biomed Eng 54(11):1965–1973

Formisano E, Esposito F, Di Salle F, Goebel R (2004) Cortex-based independent component analysis of fMRI time series. Magn Reson Imaging 22(10):1493–1504

Granger CWJ (1969) Investigating causal relations by econometric models and cross-spectral methods. Econometrica 37:424–438

Grave de Peralta Menendez R, Gonzalez Andino SL (1999) Distributed source models: standard solutions and new developments. In: Uhl C (ed) Analysis of neurophysiological brain functioning. Springer, Heidelberg, pp 176–201

Hansen PC (1992) Analysis of discrete ill-posed problems by means of L-curve. SIAM Rev 43:561–580

Hasson U, Nir Y, Levy I, Fuhrmann G, Malach R (2004) Intersubject synchronization of cortical activity during natural vision. Science 303:1634–1640

Horwitz B (2003) The elusive concept of brain connectivity. Neuroimage 19(2 Pt 1):466–470

Hsu M, Bhatt M, Adolphs R, Tranel D, Camerer CF (2005) Neural systems responding to degrees of uncertainty in human decision-making. Science 310:1680–1683

Kaminski M, Blinowska K (1991) A new method of the description of the information flow in the brain structures. Biol Cybern 65:203–210

Kaminski M, Ding M, Truccolo WA, Bressler S (2001) Evaluating causal relations in neural systems: granger causality, directed transfer function and statistical assessment of significance. Biol Cybern 85:145–157

King-Casas B, Tomlin D, Anen C, Camerer CF, Quartz SR, Montague PR (2005) Getting to know you: reputation and trust in a two-person economic exchange. Science 308(5718):78–83

Knobe J (2005) Theory of mind and moral cognition: exploring the connections. Trends Cogn Sci 9(8):357–359

Kuhnen CM, Knutson B (2005) The neural basis of financial risk taking. Neuron 47:763–770

Lancaster JL, Rainey LH, Summerlin JL, Freitas CS, Fox PT, Evans AC, Toga AW, Mazziotta JC (1997) Automated labeling of the human brain: a preliminary report on the development and evaluation of a forward-transform method. Hum Brain Mapp 5:238–242

Lancaster JL, Woldorff MG, Parsons LM, Liotti M, Freitas CS, Rainey L, Kochunov PV, Nickerson D, Mikiten SA, Fox PT

(2000) Automated Talairach Atlas labels for functional brain mapping. Hum Brain Mapp 10:120–131

Lee RB, DeVore I (eds) (1968) What hunters do for a living, or, how to make out on scarce resources. In: Man the hunter. Aldine, Chicago, pp 30–48

Montague PR, Berns GS, Cohen JD, McClure SM, Pagnoni G, Dhamala M et al (2002) Hyperscanning: simultaneous fMRI during linked social interactions. Neuroimage 16:1159–1164

Mulert C, Menzinger E, Leicht G, Pogarell O, Hegerl U (2005) Evidence for a close relationship between conscious effort and anterior cingulate cortex activity. Int J Psychophysiol 56:65–80

Nunez PL (1995) Neocortical dynamics and human EEG rhythms. Oxford University Press, New York

Oliveri M, Babiloni C, Filippi MM, Caltagirone C, Babiloni F, Cicinelli P et al (2003) Influence of the supplementary motor area on primary motor cortex excitability during movements triggered by neutral or emotionally unpleasant visual cues. Exp Brain Res 149(2):214–221

Preuschoff K, Bossaerts P, Quartz S (2006) Neural differentiation of expected reward and risk in human subcortical structures. Neuron 51:381–390

Raz J, Turetsky B, Fein G (1988) Confidence intervals for the signal-to-noise ratio when a signal embedded in noise is observed over repeated trials. IEEE Trans BME 35(8):646–649

Sanfey AG, Rilling JK, Aronson JA, Nystrom LE, Cohen JD (2003) The neural basis of economic decision-making in the Ultimatum Game. Science 300:1755–1758

Sato JR, Takahashi DY, Arcuri SM, Sameshima K, Morettin PA, Baccalà LA (2009) Frequency domain connectivity identification: an application of partial directed coherence in fMRI. Hum Brain Mapp 30(2):452–461

Schlögl A, Supp G (2006) Analyzing event-related EEG data with multivariate autoregressive parameters. Prog Brain Res 159:135–147 Review

Sporns O (2006) Small-world connectivity, motif composition, and complexity of fractal neuronal connections. Biosystems 85(1):55–64

Stephan KE, Riera JJ, Deco G, Horwitz B (2008) The Brain Connectivity Workshops: moving the frontiers of computational systems neuroscience. Neuroimage 42(1):1–9. Epub 2008 Apr 20

Taxidis J, Coomber B, Mason R, Owen M (2010) Assessing cortico-hippocampal functional connectivity under anesthesia and kainic acid using generalized partial directed coherence. Biol Cybern 102:327–340

Theiler J, Eubank S, Longtin A, Galdrikian B, Farmer JD (1992) Testing for nonlinearity in time series: the method of surrogate data. Physica D 58:77–94

Tobler PN, Fiorillo CD, Schultz W (2005) Adaptive coding of reward value by dopamine neurons. Science 307:1642–1645

Tononi G, Sporns O, Edelman GM (1994) A measure for brain complexity: relating functional segregation and integration in the nervous system. Proc Natl Acad Sci USA 91:5033–5037

Urbano A, Babiloni F, Babiloni C, Ambrosini A, Onorati P, Rossini PM (1997) Human short-latency cortical responses to somatosensory stimulation. A high resolution study. NeuroReport 8(15):3239–3243

Urbano A, Babiloni C, Carducci F, Fattorini L, Onorati P, Babiloni F (1998) Dynamic functional coupling of high resolution EEG potentials related to unilateral internally triggered one-digit movements. Electroencephalogr Clin Neurophysiol 106:477–487

Varela F, Lachaux JP, Rodriguez E, Martinerie J (2001) Thebrainweb: phase synchronization and large-scale integration. Nat Rev Neurosci 2:229–239

Walton ME, Bannerman DM, Rushworth MF (2002) The role of rat medial frontal cortex in effort-based decision making. J Neurosci 22:10996–11003

Whiten A, Byrne RW (1988) Tactical deception in primates. Behav Brain Sci 11:233–273

Yook SH, Jeong H, Barabási A, Tu Y (2001) Weighted evolving networks. Phys Rev Lett 86(25):5835–5838

Zar J (1984) Biostatistical analysis. Prentice Hall, New York